Intrinsic Polarization Super Junctions: Design of Single and Multi-Channel GaN Structures

Luca Nela, Catherine Erine, Amirmohammad Miran Zadeh, and Elison Matioli

***Abstract*- Super Junctions (SJs) have enabled unprecedented performance in Silicon power devices, which could be further improved by applying this concept to wide-band-gap semiconductors like Gallium Nitride (GaN). Currently, Polarization Super Junctions (PSJs) are the most promising candidates for GaN SJs. Yet, until now, *p*-type doping of the GaN cap layer was required to ensure the presence of a two-dimensional hole gas (2DHG), and the proper charge matching between the 2DHG and two-dimensional electron gas (2DEG), which is fundamental to the operation of super-junctions. This approach, however, requires precise control of the *p*-GaN doping level, which is very challenging and has hindered the demonstration of high-performance PSJs. Besides, while PSJs are particularly promising for multi-channel structures aimed at reducing the sheet resistance, achieving proper charge matching combined with large electron density for all the buried channels is challenging. Here, we propose a simple and robust platform for intrinsic PSJ (i-PSJ) that enables excellent charge matching for a wide range of structures, without relying on doping. We show that surface donor states are the origin of charge mismatch and provide a strategy to minimize their impact. Simulated devices based on this structure show optimal carrier depletion with a flat electric field profile in the whole drift region. Finally, we extend this concept to multi-channel i-PSJ structures. We demonstrate a much-reduced sheet resistance down to 58 Ω/sq and present a robust strategy to achieve charge balance, which enables reducing the on-resistance without degrading the off-state performance, thus greatly improving the device figure-of-merit.**

***Index terms*- Gallium Nitride, Polarization Super Junction, Power Devices, Multi-channel, Charge Balance**

I. Introduction

Silicon Super Junction (SJ) devices, which rely on the precise charge matching between *n*-type and *p*-type pillars to create a neutral depletion region while achieving high conductivity in on-state, have enabled a significant decrease of the device resistance for a certain breakdown voltage (V_{BR}), leading to performances beyond the one-dimensional Si material limit [1], [2]. As Wide-Band-Gap (WBG) semiconductors, such as GaN, are emerging, the application of the SJ concept to these better-performing materials could lead to great improvements in the state-of-the-art [3]–[7] by enabling a considerable reduction of both resistive and switching losses [3]. Yet, GaN SJs are still out of reach, hindered by the difficulties in achieving selective and highly-doped *p*-type regions because of the absence of effective Mg implantation or high-quality *p*-GaN regrowth [8], [9].

Authors are with the Power and Wide-Band-Gap Electronics Research Laboratory, École Polytechnique Fédérale de Lausanne, 1015 Lausanne, Switzerland (e-mail: luca.nela@epfl.ch, elison.matioli@epfl.ch).

This work was supported in part by the Swiss National Science Foundation through the Assistant Professor (AP) Energy under Grant PYAPP2_166901, and in part by the ECSEL Joint Undertaking (JU) under Grant 826392. The JU receives support from the European Union's Horizon 2020 Research and Innovation Program and Austria, Belgium, Germany, Italy, Norway, Slovakia, Spain, Sweden, and Switzerland

The AlGaN/GaN lateral platform offers a unique alternative to conventional vertical SJs. In these structures, a two-dimensional electron and hole gas (2DEG and 2DHG) of equal carrier concentrations (N_s and P_s respectively) can be obtained naturally without requiring any doping [10], thanks to the presence of matching polarization charges, enabling the realization of Polarization Super Junctions (PSJs) [11]–[15]. The charge balance between the 2DEG and 2DHG, and the intrinsically matched polarization charges, can result in a neutral depletion region, leading to similar off-state behavior as in conventional doping-based SJs.

Nevertheless, translating the matching polarization charges into mobile N_s and P_s of equal concentration that can be depleted during the off-state is a challenging task due to the presence of ionized donor states at the top crystal surface, which provide electrons to the 2DEG and prevent the formation of a large-density 2DHG [16], [17]. The most common strategies to address these issues comprise the use of a *p*-doped GaN cap layer to provide holes to the 2DHG [18]–[22] or the compensation between a *p*-GaN cap layer and an *n*-type delta-doped region [23]–[25]. However, the introduction of a *p*-doped cap defeats the purpose of PSJs, leading to the typical challenges in charge balancing as in conventional doped SJs, which are aggravated by the difficult *p*-GaN doping. In particular, the use of a *p*-GaN cap requires the precise control of its thickness and especially of its doping level, which is very challenging due to the inefficient Mg activation and to its thermal back diffusion [26], [27]. Besides, the strong dependence of the Mg activation on temperature [26], [27] leads to an increased carrier mismatch (Δ) when the device heats up during operation, thus resulting in an early breakdown.

Previous works [11], [13] have also claimed the demonstration of PSJ devices by employing usual AlGaN/GaN HEMTs structures without any GaN cap on top, which were referred to as natural PSJ. However, in usual AlGaN/GaN HEMTs, no 2DHG can be formed due to the presence of ionized donor states at the top crystal surface, which provide electrons to the 2DEG [10], [16], [17]. These states represent a fixed net charge contribution that imposes an electric field gradient in the drift region and hinders any super junction effect. Finally, PSJ devices based on 3D polarization doping have also been proposed [12], [28]. Yet, these devices require a challenging control of the growth parameters to ensure a very precise $Al_xGa_{1-x}N$ graded profile over thick layers and suffer from reduced carrier mobility due to the strong alloy scattering.

To address these limitations, in this work, we propose a simple and robust platform for intrinsic PSJ (i-PSJ) based on a thick undoped GaN cap layer, which enables to achieve charge balancing regardless of the surface and temperature conditions, without any need for precisely controlled doping.

Although heterostructures with undoped GaN cap were reported [15], [16], [29] and the presence of a 2DHG was shown experimentally [26], [27], [30], these studies did not focus on the design of i-PSJs. Thus, key challenges of these structures such as achieving a small charge mismatch regardless of surface donor states and obtaining large N_s despite the thick cap remain unexplored [15]. Here, we show that by employing a thick undoped GaN cap excellent intrinsic matching between N_s and P_s is obtained and maintained for any surface condition while still achieving a large 2DEG density. Simulated devices based on this heterostructure show the typical SJ behavior with a neutral drift region, which results in an ideal constant off-state electric field. The effect of donor states at the GaN top surface on the carrier mismatch is discussed and the role of the charge imbalance on the device performance is presented.

Besides, to significantly reduce the device on-resistance, we investigate intrinsic multi-channel PSJs, in which several channels are stacked to decrease the heterostructure sheet resistance. In particular, we address the main challenges of these structures, namely the population of all the buried channels and charge matching. Multi-channel structures typically employ doping of the barrier to increase the carrier concentration in the buried channels [31]–[33]. This strategy however results in fixed donor charges in the off-state and is thus not suitable for PSJs. Another possibility consists of including both *n*-type doping in the barrier and *p*-type doping in the GaN channel to balance the fixed charges [23]. Yet, this approach is very difficult to implement in GaN devices due to the strong Mg memory effect and inefficient activation, which prevent an accurate control of the doping level, resulting in a large charge mismatch. In addition, it should be noted that charge matching for all of the channels, including the top and bottom ones, should be achieved as any charge mismatch would limit the breakdown voltage of the device [13].

Here, we propose an intrinsic multi-channel structure with a thick undoped GaN cap as an optimal platform for multi-channel i-PSJs. We demonstrate that large carrier densities and reduced sheet resistance can be achieved also for intrinsic multi-channels and we present a robust strategy to achieve proper charge balance in multi-channel structures. Simulated devices based on this approach show a flat off-state electric field profile despite the increased carrier density and thus have the potential to greatly improve Baliga's figure-of-merit.

II. Design of Single-Channel Heterostructures

The first step to designing a charge-balanced heterostructure is to identify the source of the electrons in the 2DEG. Indeed, while at equilibrium charge neutrality is always guaranteed in the structure, during the off-state mobile electrons are depleted by the high voltage. If these electrons have been generated by the formation of other mobile carriers (e.g. holes), these can also be depleted, resulting in a neutral drift region and in a SJ behavior. However, if the source of the 2DEG is fixed charges, such as surface donor states, these cannot be depleted and result in a net charge contribution in the drift region, thus affecting the off-state electric field as in conventional doping-based devices.

Figure 1 (a) shows the investigated heterostructure which comprises a GaN channel, an AlGaN barrier, and a GaN un-

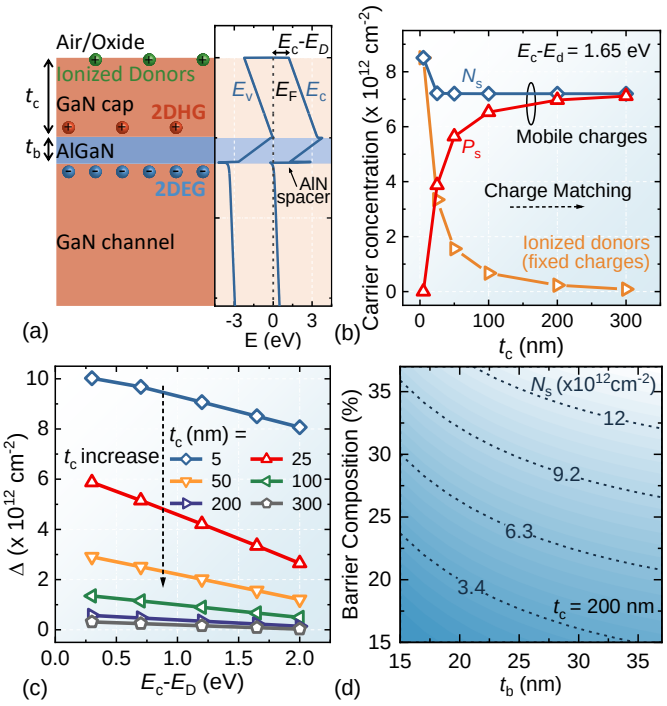

Fig. 1. (a) Investigated heterostructure and corresponding band structure. (b) N_s, P_s, and ionized donors as a function of the GaN cap thickness (t_c) (c) Carrier mismatch (Δ) as a function of the donor states energy for different t_c (d) N_s as a function of the AlGaN barrier thickness and composition for a 200 nm-thick GaN cap.

doped cap. This results in a 2DEG at the bottom GaN/AlGaN interface and, depending on the conditions, in a 2DHG at the top GaN/AlGaN interface. Donor states with an energy level E_D are located at the GaN cap/insulator interface due to the presence of the crystal surface. While the structure is similar to conventional GaN HEMT heterostructures, increasing the undoped GaN cap thickness (t_c) enables to reach charge matching between 2DEG and 2DHG, which offers an excellent platform for intrinsic PSJs.

Typical HEMT heterostructures employ a very thin (~2-3 nm) GaN cap, whose main purpose is to protect the AlGaN barrier during processing. In this case, the N_s in the 2DEG is entirely generated by ionized surface donor states [16], [17] (Fig. 1 (a-b)). While electrons in the 2DEG are mobile charges that are depleted during the off-state, ionized surface donors are fixed positive charges that remain in the depleted region and directly affect the field profile in the off-state. Thus, while the presence of matching polarization charges is a necessary condition for PSJs, this is not sufficient to achieve any super junction effect in conventional HEMT structures. In particular, the key mechanism lies in translating the matched polarization charges into a mobile 2DHG and 2DEG of equal concentration. In this case, the N_s in the 2DEG is entirely generated by mobile holes in the 2DHG that can be depleted in the off-state, resulting in a neutral drift region. This favorable condition can be achieved by adjusting the GaN cap thickness. As t_c increases, more and more electrons in the 2DEG originate from the valence band at the top AlGaN interface, rather than from ionized surface donor traps, forming a 2DHG with hole concentration P_s (Fig. 1(b)). The difference between the mobile N_s and P_s, i.e. the charge mismatch $\Delta=N_s-P_s$, corresponds to the density of ionized

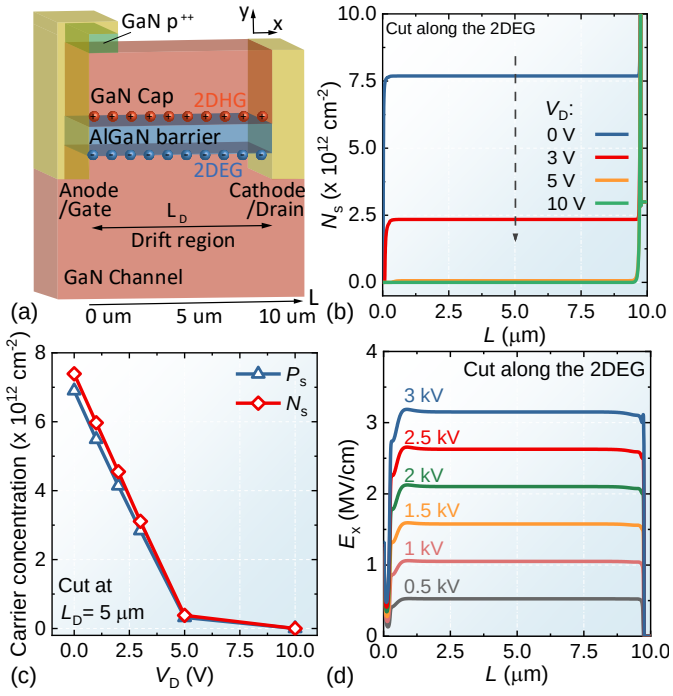

Fig. 2. (a) Schematic of the drift region of an i-PSJ device (b) N_s profile at the AlGaN/GaN bottom interface as a function of the reverse voltage (c) N_s and P_s cut in the middle of the drift region as a function of V_D (d) E_x profile at the AlGaN/GaN bottom interface for different V_D.

donor states at the top GaN cap surface (Fig. 1(b)) and is a direct indicator of the net fixed charges in the depleted part of the device's drift region during the off-state. For large thicknesses of the cap, P_s further increases and approaches very closely the N_s value, leading to an intrinsic negligible charge mismatch (Fig. 1 (b)). It should be noted that, while it is important to achieve P_s and N_s of matching concentrations to minimize Δ, the impact of holes on the heterostructure conductivity is negligible due to their much lower mobility compared to electrons in the 2DEG [26], [30], [34], [35].

In the absence of a top metal, the Fermi level at the GaN surface is determined by the energy level of the donor traps [17]. While experimental values are present in the literature [16], [17], the exact E_D (or its distribution) highly depends on the surface conditions, which are unpredictable and can influence the Δ value. Figure 1 (c) shows that a considerable dependence of Δ on the trap energy is present for small t_c, which however becomes negligible as t_c increases. This allows achieving a minimal carrier mismatch regardless of the presence of top donor states, thus preventing any influence from the surface conditions on Δ. The reduced impact of the surface states on the 2DHG concentration, and thus on Δ, can also be seen as an electrostatic screening effect that increases with larger GaN cap thicknesses. Despite the presence of a thick cap layer (t_c = 200 nm), large N_s values can still be obtained by employing realistic barrier thicknesses and compositions (Fig. 1 (d)), which makes the proposed heterostructure an excellent and robust platform for intrinsic PSJs.

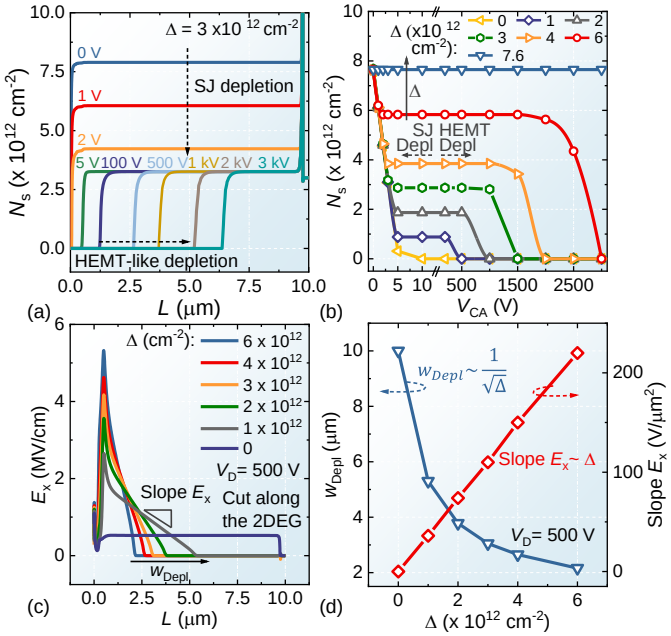

Fig. 3. (a) N_s profile as a function of V_D for a PSJ device with Δ of 3 x 10^{12} cm^{-2} for different V_D. (b) Cut of the N_s concentration at L_D = 5μm as a function of V_D and Δ (c) E_x profile for V_D =500 V for different mismatch values. (d) w_{Depl} and slope of E_x as a function of Δ for V_D =500 V.

III. Single Channel i-PSJ Devices

To understand the potential of charge balance to improve the off-state electric field distribution, we focus our analysis on the drift region of an i-PSJ device. It should be noted that the carrier depletion and electric field in the drift region are equivalent for a diode and a transistor (with the anode corresponding to the gate and the cathode to the drain). Therefore, the proposed concept and analysis are general and valid for both types of devices. The heterostructures comprises a 30 nm-thick $Al_{0.25}GaN$ barrier, and a 200 nm-thick UID cap (Fig. 2 (a)), leading to N_s of 0.8 x 10^{13} cm^{-2} and Δ < 0.3 x 10^{12} cm^{-2}. A first electrode (cathode or drain) with work-function (Φ_b) of 4.2 eV provides ohmic contact to the 2DEG and Schottky contact to the 2DHG, while a second electrode (anode or gate) (Φ_b=5.2 eV) provides a barrier to electrons in the 2DEG. A top ohmic contact to the 2DHG is realized by a p^{++} GaN layer (whose aim is only to improve the contact to the 2DHG but has no role in the charge matching) and a metal electrode [34], which is connected to the anode or gate. Good contact to the 2DHG is important for an efficient depletion and injection of holes and is required to avoid any degradation during high-frequency switching, as shown in [23]. The p^{++}-GaN layer can be either grown during the heterostructure epitaxy and then removed in the access region or realized by other techniques under development such as selective area regrowth [36]–[38] or ion implantation [39]–[41]. The device simulation was performed using Silvaco Atlas software and employing its built-in material parameters [42].

Contrary to conventional devices in which the charge depletion in the off-state extends from the anode (or gate) towards to cathode (or drain), the intrinsic PSJ device shows a uniform and simultaneous depletion of the 2DEG in the whole drift region (L_D) (Fig. 2 (b)). Most importantly, a full carrier depletion is achieved at an extremely low voltage over the drift

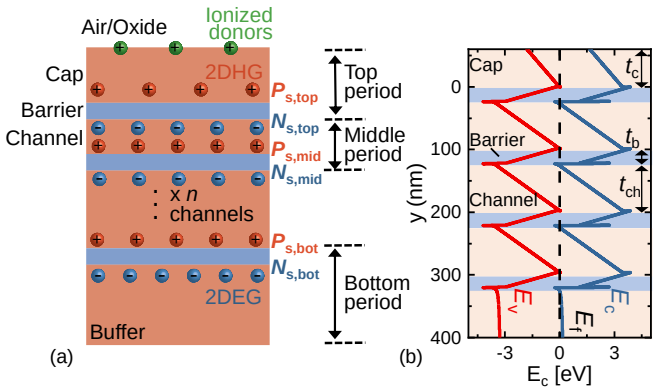

Fig. 4. (a) Cross-sectional schematic and (b) bandstructure of the multi-channel heterostructure under study.

region (V_D) of ~ 5 V, with the same behavior for both N_s and P_s (Fig. 2 (c)). This results in an electric field profile that is flat along the whole drift region (Fig. 2 (d)), which is a clear feature of SJs and allows to significantly increase the device V_{BR}.

Unbalanced structures were investigated to determine the effect of the carrier mismatch on the device performance. Ionized surface states with the density shown in Fig. 1 (c) were introduced at the top GaN cap interface, resulting in the desired fixed net charge contribution. Figure 3 (a) shows the carrier depletion for a PSJ device having $\Delta \sim 3 \times 10^{12}$ cm^{-2}. Two different processes can be identified: first, the device behaves as a PSJ with a uniform carrier depletion down to a level limited by the value of Δ for V_D of only a few Volts (Fig. 3 (b)). Beyond this point, conventional depletion occurs, as in the case of typical HEMT-like devices, which grows from the anode (or gate) to the cathode (or drain) and requires very large V_D values to expand. This results in a degradation of the off-state field distribution, and thus of the blocking performance, as the mismatch increases (Fig. 3 (c)). The depletion width (w_{Depl}) reduces and the E_x slope rises as Δ increases, leading to the typical triangular shape of the electric field in conventional HEMT structures. Besides, it is possible to observe that $w_{Depl} \sim 1/\sqrt{\Delta}$ and the slope of $E_x \sim \Delta$ (Fig. 3 (d)), which is the typical behavior of conventional HEMTs and shows that unmatched PSJs behave as a HEMT device having $N_s = \Delta$. It should be noted that under large off-state bias electron injection to the positively-charged ionized surface states can mitigate the net charge contribution and thus locally reduce Δ. This is referred to as to virtual gate effect and can result in a smoothening of the electric field peak at the gate/anode edge [43]–[46]. However, this mechanism also leads to severe current collapse [47], [48] due to the time required for the electrons de-trapping, and thus it is highly undesirable. On the contrary, additional ionization of neutral (at equilibrium) donor states during the off-state increasing Δ is not observed experimentally in the literature and thus has not been considered in this work.

The effect of Δ on the device off-state behavior does not depend on the origin of the mismatch. Thus, the presented analysis can be also employed to account for other sources of mismatch, such as possible impurities in the GaN layers, which have not been directly included in the simulation due to their strong dependence on the growth technique and parameters.

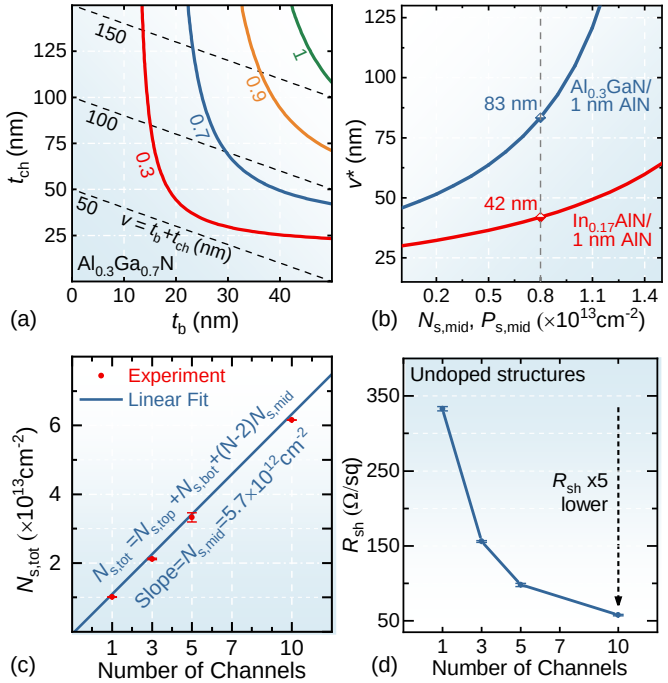

Fig. 5. (a) $N_{s,mid}$ as a function of the barrier and GaN channel thickness for an intrinsic multi-channel heterostructure with an $Al_{0.3}GaN$ barrier and 1 nm thick AlN interlayer. (b) Minimum possible period thickness for the middle channels as a function of the desired carrier density. (c) Total electron concentration and (d) sheet resistance as function of the number of channels for the grown multi-channel structures.

IV. Design of Multi-Channel Heterostructures

Since for charge-balanced intrinsic PSJs N_s can be decoupled from the off-state electric field, reducing the sheet resistance (R_{sh}) of conventional single-channel heterostructure would in principle improve the performance of the device. However, a significant R_{sh} reduction in such structures is challenging to achieve due to the trade-off between the carrier concentration and mobility [31], [32]. Multi-channel heterostructures [31], [32], [49]–[52] having multiple stacked AlGaN/GaN layers allow overcoming this limitation by distributing a large N_s in several parallel 2DEGs [31], [32]. However, two main challenges need to be addressed to achieve multi-channel intrinsic polarization super junctions. The first one consists of achieving a large carrier density in the buried channels without employing *n*-type doping of the barrier, which would result in fixed donor charges in the off-state. The second challenge is to obtain a charge-balanced structure without relying on the doping of the GaN channels [23]. The absence of *p*-type doping in the GaN layers is fundamental since the strong Mg memory effect, observed in GaN *p*-doping, would be very detrimental to the charge balance and the electron mobility due to the increased carrier scattering. Besides, charge matching for all of the channels is a fundamental requirement to achieve an effective super-junction depletion since any charge mismatch would limit the device voltage blocking capability.

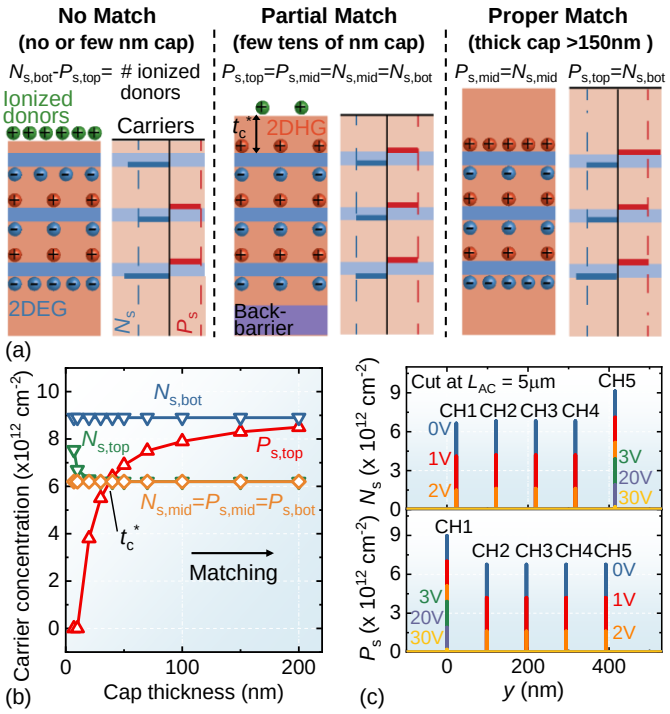

Fig. 6. (a) Different matching strategies for an intrinsic multi-channel heterostructures (b) Electrons and holes concentration in the different channels as a function of the GaN cap thickness (c) N_s and P_s depletion in the 5 channels i-PSJ device as a function of V_D.

V. Large N_s in Multi-Channel i-PSJs

The proposed intrinsic multi-channel structure with a top GaN cap is shown in Figure 4 (a), with the corresponding bandstructure reported in Figure 4 (b). In general, a multi-channel stack comprises a top and bottom channel, and n middle channels. While the 2DEG concentration of the bottom channel is similar to the single-channel case, and thus is typically large, particular care should be taken to populate the 2DEGs of the middle and top channels due to the finite thickness of the GaN channel. In the absence of n-type doping, the electron concentration in these channels ($N_{s,top}$ and $N_{s,mid}$ (Fig. 4 (a)) depends both on the barrier and GaN channel thickness (t_b and t_{ch}). A proper combination of t_b and t_{ch} should be selected to achieve the desired electron concentration and avoid unpopulated channels [53]. This sets a corresponding channel period ($v = t_b + t_{ch}$), determining the total heterostructures thickness (Fig. 5 (a)), which should be minimized to facilitate the device fabrication. By knowing the dependence of $N_{s,mid}$ on t_b and t_{ch}, the minimum possible period (v^*) to achieve a certain electron concentration can be calculated. Limitations in the maximum achievable barrier thickness could result in a slight increase of this lower bound. Figure 5 (b) shows that for a conventional $Al_{0.3}GaN$ barrier with a 1 nm-thick AlN interlayer, v^* could be of about 80 nm to reach a large $N_{s,mid}$ of 8 x 10^{12} cm^{-2} in the middle channels. Besides, v^* can be further reduced by employing a higher polarization barrier material such as $In_{0.17}AlN$, which leads to a twofold reduction of v^* compared to $Al_{0.3}GaN$, enabling to stack more channels and increase the total electron concentration ($N_{s,tot}$).

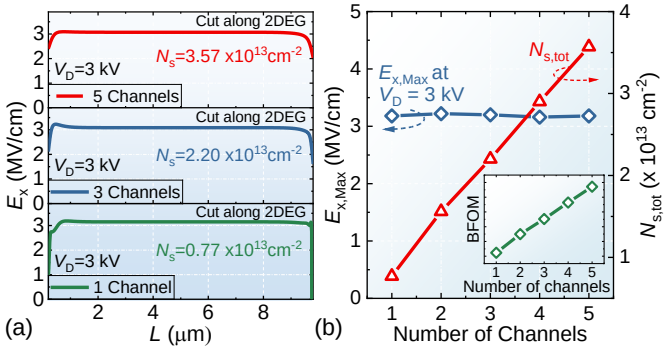

Fig. 7. (a) Off-state E_x profile for a 1-,3-, and 5- channel i-PSJ device. (b) Maximum E_x and N_s as a function of the number of channels. The inset shows the linear growth of Baliga's figure-of-merit (BFOM) with the number of channels.

The feasibility of this approach based on undoped layers was experimentally verified growing by MOCVD intrinsic multi-channel heterostructures with a different number of channels, each comprising a 23 nm $Al_{0.3}GaN$ barrier, a 0.8 nm AlN spacer, and a 75 nm GaN channel. The growth temperature was 1050 °C for the GaN channels and 1030 °C for the AlGaN barriers while the pressure was set to 200 mbar and 150 mbar, respectively. H_2 carrier gas and TMGa and TMAl precursors were used. A linear increase of $N_{s,tot}$ with the number of channels is observed, which confirms the successful population of all the middle channels with an $N_{s,mid}$ of about 6 x 10^{12} cm^{-2} (Fig. 5 (c)). This enables a significant enhancement of total electron density as the number of channels is increased, thus resulting in a large reduction of the sheet resistance from 340 Ω/sq for a single channel down to about 58 Ω/sq for a 10-channel structure, even without employing any n-type doping of the barrier (Fig. 5 (d)).

VI. Charge Matching in Multi-Channel i-PSJs

The charge-balancing approach based on a thick GaN cap proposed for single-channel devices can also be applied to multi-channel structures to realize multi-channel intrinsic PSJs. Besides, in the absence of doping, the N_s and P_s of the buried middle channels are intrinsically matched because of charge conservation, i.e. $P_{s,mid} = N_{s,mid}$. However, charge matching for all of the channels, including especially also the top and bottom channels, is required to achieve an effective super-junction depletion. While a GaN cap is always necessary to ensure the presence of the top 2DHG ($P_{s,top}$) (Fig. 6 (a)), as in the case of a single-channel, two different strategies can be investigated for multi-channel structures.

1) One can set all the N_s and P_s to be equal for all channels, i.e. $P_{s,top} = N_{s,top} = P_{s,mid} = N_{s,mid} = P_{s,bot} = N_{s,bot}$. To this end, the thickness of the GaN cap should be properly designed (t_c^* in Fig. 6 (b)) to achieve $P_{s,top} = P_{s,mid}$, as very thick GaN cap layers would result in an excess of holes (Fig. 6 (a-b)). In addition, $N_{s,bot}$ should be reduced to match the concentration of the middle channels by employing, for instance, a back-barrier layer (Fig. 6 (a)). However, in this approach, the small cap thickness still results in ionized surface donors at the top surface (as shown in Fig. 1 (b)). This leads to a fixed net charge contribution preventing proper charge matching with this strategy.

2) A second possibility consists of matching the top 2DHG and the bottom 2DEG independently from the middle channels, i.e. $P_{s,top} = N_{s,bot}$ and $N_{s,top} = P_{s,mid} = N_{s,mid} = P_{s,bot}$. In this case, the GaN cap just needs to be thick enough, as in the single-channel case, and no back-barrier is required (Fig. 6 (a-b)). This method is more robust since the thick GaN cap prevents the ionization of surface donor states (Fig. 1 (b)) and no precise tuning of the back-barrier is required.

A multi-channel i-PSJ based on this structure was simulated to investigate the off-state performance of a charge-balanced multi-channel device. The multi-channel stack herein investigated comprises 5 channels with a 23 nm-thick $Al_{0.3}GaN$ barrier, a 75 nm-thick GaN channel, and a 200 nm-thick GaN cap. This is structure is similar to the ones presented in Fig. 5 (c-d) and in [51] showing the feasibility of such an approach. Intrinsic PSJ multi-channel devices based on this structure show a two-step depletion of the drift region. Depletion of all of the carriers in the middle channels occurs first at a V_D of ~ 3 V (Fig. 6 (c)), followed by the depletion of the top 2DHG and bottom 2DEG, which have a higher carrier concentration, at V_D of ~ 30 V (Fig. 6 (c)). Since a full carrier depletion is achieved at very low reverse voltage, similarly to the single-channel case, a flat E_x profile is obtained in the whole drift region (Fig. 7 (a)). Most importantly, due to the efficient PSJ carrier depletion, the electric field value is independent of N_s. Therefore N_s can be significantly increased by adding more channels without affecting the device breakdown (Fig. 7 (b)). This results in linear growth of Baliga's figure-of-merit as the number of channels is increased (inset in Fig. 7 (b)), potentially overcoming the 1D GaN materials' limit and leading to a great improvement in the performance of GaN power devices.

VII. Conclusion

In this work, we proposed a simple and robust approach to realize both single- and multi-channel intrinsic PSJ without any need for a *p*-GaN cap layer and precisely controlled doping level. Excellent intrinsic matching between was achieved and maintained for any surface condition, thus providing a robust platform for i-PSJs. An i-PSJ device based on this approach was simulated and showed the typical SJ behavior with an ideal constant electric field in the whole drift region. The effect of donor states at the GaN top surface on the carrier mismatch was discussed and its influence on the device performance minimized. Finally, we extended this concept to intrinsic multi-channel structures, showing that much-reduced sheet resistance and excellent charge matching can be achieved simultaneously. Simulated devices based on this approach showed a flat off-state electric field profile despite the increased carrier density and thus have the potential to greatly improve Baliga's figure-of-merit.

References

[1] T. Fujihira, "Theory of Semiconductor Superjunction Devices," *Jpn. J. Appl. Phys.*, vol. 36, pp. 6254–6262, 1997.

[2] F. Udrea, G. Deboy, and T. Fujihira, "Superjunction power devices, history, development, and future prospects," *IEEE Trans. Electron Devices*, vol. 64, no. 3, pp. 720–734, 2017, doi: 10.1109/TED.2017.2658344.

[3] L. Nela, C. Erine, M. V. Oropallo, and E. Matioli, "Figures-of-Merit of Lateral GaN Power Devices : modeling and comparison of HEMTs and PSJs," *IEEE J. Electron Devices Soc.*, vol. 9, pp. 1066–1075, 2021.

[4] X. Zhou, J. R. Howell-Clark, Z. Guo, C. W. Hitchcock, and T. P. Chow, "Performance limits of vertical GaN of conventional doped pn and natural polarization superjunction devices," *Appl. Phys. Lett.*, vol. 115, no. 11, 2019, doi: 10.1063/1.5109389.

[5] R. Chu, "GaN power switches on the rise: Demonstrated benefits and unrealized potentials," *Appl. Phys. Lett.*, vol. 116, no. 9, 2020, doi: 10.1063/1.5133718.

[6] H. Huang, J. Cheng, B. Yi, W. Zhang, and W. T. Ng, "A unified model for vertical doped and polarized superjunction GaN devices," *Appl. Phys. Lett.*, vol. 116, no. 10, 2020, doi: 10.1063/1.5142855.

[7] M. Meneghini, C. De Santi, I. Abid, M. Buffolo, M. Cioni, R. A. Khadar, L. Nela, N. Zagni, A. Chini, F. Medjdoub, G. Meneghesso, G. Verzellesi, E. Zanoni, and E. Matioli, "GaN-based power devices : physics , reliability and perspectives," *J. Appl. Phys.*, vol. 130, no. 16, p. 227, 2021, doi: 10.1063/5.0061354.

[8] T. Zhang, J. Zhang, H. Zhou, Y. Wang, T. Chen, K. Zhang, Y. Zhang, K. Dang, Z. Bian, J. Zhang, S. Xu, X. Duan, J. Ning, and Y. Hao, "A > 3 kV/2.94 m Ω cm2 and Low Leakage Current with Low Turn-On Voltage Lateral GaN Schottky Barrier Diode on Silicon Substrate with Anode Engineering Technique," *IEEE Electron Device Lett.*, vol. 40, no. 10, pp. 1583–1586, 2019, doi: 10.1109/LED.2019.2933314.

[9] E. V. S. Hemt, Z. Li, S. Member, and T. P. Chow, "Design and Simulation of 5–20-kV GaN Enhancement-Mode Vertical Superjunction HEMT," *IEEE Trans. Electron Devices*, vol. 60, no. 10, pp. 3230–3237, 2013, doi: 10.1109/TED.2013.2266544.

[10] J. D. Wood Colin, *Polarization effects in Semiconductors*. 2008, doi: 10.1016/0370-2693(87)90376-5.

[11] H. Ishida, D. Shibata, M. Yanagihara, Y. Uemoto, H. Matsuo, T. Ueda, T. Tanaka, and D. Ueda, "Unlimited high breakdown voltage by natural super junction of polarized semiconductor," *IEEE Electron Device Lett.*, vol. 29, no. 10, pp. 1087–1089, 2008, doi: 10.1109/LED.2008.2002753.

[12] B. Song, M. Zhu, Z. Hu, K. Nomoto, D. Jena, and H. Xing, "Design and optimization of GaN lateral polarization-doped super-junction (LPSJ): An analytical study," *Proc. Int. Symp. Power Semicond. Devices ICs*, pp. 273–276, 2015, doi: 10.1109/ISPSD.2015.7123442.

[13] H. Ishida, D. Shibata, H. Matsuo, M. Yanagihara, Y. Uemoto, T. Ueda, T. Tanaka, and D. Ueda, "GaN-based natural super junction diodes with multi-channel structures," *Tech. Dig. - Int. Electron Devices Meet. IEDM*, 2008, doi: 10.1109/IEDM.2008.4796636.

[14] A. Nakajima, K. Adachi, M. Shimizu, and H. Okumura, "Improvement of unipolar power device performance using a polarization junction," *Appl. Phys. Lett.*, vol. 89, no. 19, pp. 87–90, 2006, doi: 10.1063/1.2372758.

[15] H. Kawai, S. Yagi, S. Hirata, F. Nakamura, T. Saito, Y. Kamiyama, M. Yamamoto, H. Amano, V. Unni, and E. M. S. Narayanan, "Low cost high voltage GaN polarization superjunction field effect transistors," *Phys. Status Solidi Appl. Mater. Sci.*, vol. 214, no. 8, 2017, doi: 10.1002/pssa.201600834.

[16] S. Heikman, S. Keller, Y. Wu, J. S. Speck, S. P. DenBaars, and U. K. Mishra, "Polarization effects in AlGaN/GaN and GaN/AlGaN/GaN heterostructures," *J. Appl. Phys.*, vol. 93, no. 12, pp. 10114–10118, 2003, doi: 10.1063/1.1577222.

[17] J. P. Ibbetson, P. T. Fini, K. D. Ness, S. P. DenBaars, J. S. Speck, and U. K. Mishra, "Polarization effects, surface states, and the source of electrons in AlGaN/GaN heterostructure field effect transistors," *Appl. Phys. Lett.*, vol. 77, no. 2, 2000, doi: 10.1063/1.126940.

[18] A. Nakajima, Y. Sumida, M. H. Dhyani, H. Kawai, and E. M. Narayanan, "GaN-based super heterojunction field effect transistors using the polarization junction concept," *IEEE Electron Device Lett.*, vol. 32, no. 4, pp. 542–544, 2011, doi: 10.1109/LED.2011.2105242.

[19] B. Shankar and M. Shrivastava, "Safe Operating Area of Polarization Super-junction GaN HEMTs and Diodes," *IEEE Trans. Electron Devices*, vol. 66, no. 10, pp. 4140–4147, 2019, doi: 10.1109/TED.2019.2933362.

[20] S. Sharbati, T. Ebel, and W. T. Franke, "Design of E-mode GaN HEMTs by the Polarization Super Junction (PSJ) technology,"

Microelectron. Reliab., vol. 114, p. 113907, 2020, doi: 10.1016/j.microrel.2020.113907.

[21] M. Xiao, Y. Ma, K. Liu, K. Cheng, and Y. Zhang, "10 kV, 39 mΩ·cm2Multi-Channel AlGaN/GaN Schottky Barrier Diodes," *IEEE Electron Device Lett.*, vol. 42, no. 6, pp. 808–811, 2021, doi: 10.1109/LED.2021.3076802.

[22] H. Hahn, B. Reuters, S. Geipel, M. Schauerte, F. Benkhelifa, O. Ambacher, H. Kalisch, and A. Vescan, "Charge balancing in GaN-based 2-D electron gas devices employing an additional 2-D hole gas and its influence on dynamic behaviour of GaN-based heterostructure field effect transistors," *J. Appl. Phys.*, vol. 117, no. 10, 2015, doi: 10.1063/1.4913857.

[23] S. Han, J. Song, and R. Chu, "Design of GaN/AlGaN/GaN Super-Heterojunction Schottky Diode," *IEEE Trans. Electron Devices*, vol. 67, no. 1, pp. 69–74, 2020, doi: 10.1109/TED.2019.2953843.

[24] S. W. Han, J. Song, S. H. Yoo, Z. Ma, R. M. Lavelle, D. W. Snyder, J. M. Redwing, T. N. Jackson, and R. Chu, "Experimental Demonstration of Charge- Balanced GaN Super-Heterojunction Schottky Barrier Diode Capable of 2.8 kV Switching," *IEEE Electron Device Lett.*, vol. 41, no. 12, pp. 1758–1761, 2020, doi: 10.1109/LED.2020.3029619.

[25] S. W. Han, J. Song, M. Sadek, A. Molina, M. A. Ebrish, S. E. Mohney, T. J. Anderson, and R. Chu, "12.5 kV GaN Super-Heterojunction Schottky Barrier Diodes," *IEEE Trans. Electron Devices*, pp. 2–7, 2021, doi: 10.1109/TED.2021.3111543.

[26] A. Nakajima, P. Liu, M. Ogura, T. Makino, K. Kakushima, S. I. Nishizawa, H. Ohashi, S. Yamasaki, and H. Iwai, "Generation and transportation mechanisms for two-dimensional hole gases in GaN/AlGaN/GaN double heterostructures," *J. Appl. Phys.*, vol. 115, no. 15, 2014, doi: 10.1063/1.4872242.

[27] P. Liu, K. Kakushima, H. Iwai, A. Nakajima, T. Makino, M. Ogura, S. Nishizawa, and H. Ohashi, "Characterization of two-dimensional hole gas at GaN/AlGaN heterointerface," *1st IEEE Work. Wide Bandgap Power Devices Appl. WiPDA 2013 - Proc.*, pp. 155–158, 2013, doi: 10.1109/WiPDA.2013.6695585.

[28] B. Song, M. Zhu, Z. Hu, E. Kohn, D. Jena, and H. G. Xing, "GaN lateral PolarSJs: Polarization-doped super junctions," *Device Res. Conf. - Conf. Dig.*, pp. 99–100, 2014, doi: 10.1109/DRC.2014.6872316.

[29] N. Al Mustafa, R. Granzner, V. M. Polyakov, J. Racko, M. Mikolášek, J. Breza, and F. Schwierz, "The coexistence of two-dimensional electron and hole gases in GaN-based heterostructures," *J. Appl. Phys.*, vol. 111, no. 4, 2012, doi: 10.1063/1.3688219.

[30] R. Chaudhuri, S. J. Bader, Z. Chen, D. A. Muller, H. G. Xing, and D. Jena, "A polarization-induced 2D hole gas in undoped gallium nitride quantum wells," *Science (80-.).*, vol. 365, pp. 1454–1457, 2019.

[31] L. Nela, C. Erine, P. Xiang, V. Tileli, T. Wang, K. Cheng, and E. Matioli, "Multi-channel nanowire devices for efficient power conversion," *Nat. Electron.*, vol. 4, pp. 284–290, 2021, doi: 10.1038/s41928-021-00550-8.

[32] J. Ma, C. Erine, M. Zhu, L. Nela, P. Xiang, K. Cheng, and E. Matioli, "1200 V Multi-Channel Power Devices with 2.8 Ω·mm ON-Resistance," *2019 IEEE Int. Electron Devices Meet.*, 2019, doi: 10.1109/IEDM19573.2019.8993536.

[33] J. Ma, C. Erine, P. Xiang, K. Cheng, and E. Matioli, "Multi-channel tri-gate normally-on / off AlGaN / GaN MOSHEMTs on Si substrate with high breakdown voltage and low ON-resistance," *Appl. Phys. Lett.*, vol. 113, no. 242102, pp. 1–5, 2018, doi: 10.1063/1.5064407.

[34] Z. Zheng, W. Song, L. Zhang, S. Yang, J. Wei, and K. J. Chen, "High ION and ION/IOFF Ratio Enhancement-Mode Buried p-Channel GaN MOSFETs on p-GaN Gate Power HEMT Platform," *IEEE Electron Device Lett.*, vol. 41, no. 1, pp. 26–29, 2020, doi: 10.1109/LED.2019.2954035.

[35] N. Chowdhury, Q. Xie, M. Yuan, K. Cheng, H. W. Then, and T. Palacios, "Regrowth-Free GaN-Based Complementary Logic on a Si Substrate," *IEEE Electron Device Lett.*, vol. 41, no. 6, pp. 820–823, 2020, doi: 10.1109/LED.2020.2987003.

[36] M. Xiao, Z. Du, J. Xie, E. Beam, X. Yan, K. Cheng, H. Wang, Y. Cao, and Y. Zhang, "Lateral p-GaN/2DEG junction diodes by selective-area p-GaN trench-filling-regrowth in AlGaN/GaN," *Appl. Phys. Lett.*, vol. 116, no. 5, 2020, doi: 10.1063/1.5139906.

[37] Y. Zhong, Q. Sun, H. Yang, S. Su, X. Chen, Y. Zhou, J. He, H. Gao, X. Zhan, X. Guo, and J. Liu, " Normally-off HEMTs With Regrown p-GaN Gate and Low-Pressure Chemical Vapor Deposition SiN x Passivation by Using an AlN Pre-Layer ," *IEEE Electron Device Lett.*, vol. 40, no. 9, pp. 1495–1498, 2019, doi: 10.1109/led.2019.2928027.

[38] K. Fu, H. Fu, X. Huang, H. Chen, T. H. Yang, J. Montes, C. Yang, J. Zhou, and Y. Zhao, "Demonstration of 1.27 kV Etch-Then-Regrow GaN p-n Junctions with Low Leakage for GaN Power Electronics," *IEEE Electron Device Lett.*, vol. 40, no. 11, pp. 1728–1731, 2019, doi: 10.1109/LED.2019.2941830.

[39] T. Narita, H. Yoshida, K. Tomita, K. Kataoka, H. Sakurai, M. Horita, M. Bockowski, N. Ikarashi, J. Suda, T. Kachi, and Y. Tokuda, "Progress on and challenges of p-type formation for GaN power devices," *J. Appl. Phys.*, vol. 128, no. 9, 2020, doi: 10.1063/5.0022198.

[40] B. N. Feigelson, T. J. Anderson, M. Abraham, J. A. Freitas, J. K. Hite, C. R. Eddy, and F. J. Kub, "Multicycle rapid thermal annealing technique and its application for the electrical activation of Mg implanted in GaN," *J. Cryst. Growth*, vol. 350, no. 1, pp. 21–26, 2012, doi: 10.1016/j.jcrysgro.2011.12.016.

[41] H. Sakurai, M. Omori, S. Yamada, Y. Furukawa, H. Suzuki, T. Narita, K. Kataoka, M. Horita, M. Bockowski, J. Suda, and T. Kachi, "Highly effective activation of Mg-implanted p-type GaN by ultra-high-pressure annealing," *Appl. Phys. Lett.*, vol. 115, no. 14, pp. 1–6, 2019, doi: 10.1063/1.5116866.

[42] Joachim Piprek, *Nitride Semiconductor Devices -Principles and Simulation*. 2007.

[43] A. Nakajima, S. Yagi, M. Shimizu, and H. Okumura, "Effect of deep trap on breakdown voltage in AlGaN/GaN HEMTs," *Mater. Sci. Forum*, vol. 600–603, pp. 1345–1348, 2009, doi: 10.4028/www.scientific.net/msf.600-603.1345.

[44] L. Zhu, J. Wang, H. Jiang, H. Wang, W. Wu, Y. Zhou, and G. Dai, "Theoretical analysis of buffer trapping effects on off-state breakdown between gate and drain in AlGaN/GaN HEMTs," *Proc. 2016 IEEE Int. Conf. Integr. Circuits Microsystems, ICICM 2016*, pp. 33–36, 2017, doi: 10.1109/ICAM.2016.7813558.

[45] A. M. Wells, M. J. Uren, R. S. Balmer, K. P. Hilton, T. Martin, and M. Missous, "Direct demonstration of the 'virtual gate' mechanism for current collapse in AlGaN/GaN HFETs," *Solid. State. Electron.*, vol. 49, no. 2, pp. 279–282, 2005, doi: 10.1016/j.sse.2004.10.003.

[46] R. Vetury, N. Q. Zhang, S. Keller, and U. K. Misha, "The impact of surface states on the DC and RF characteristics of AlGaN/GaN HFETs," *IEEE Trans. Electron Devices*, vol. 48, no. 3, pp. 560–566, 2001, doi: 10.1109/16.906451.

[47] T. Hashizume, K. Nishiguchi, S. Kaneki, J. Kuzmik, and Z. Yatabe, "State of the art on gate insulation and surface passivation for GaN-based power HEMTs," *Mater. Sci. Semicond. Process.*, vol. 78, pp. 85–95, 2018, doi: 10.1016/j.mssp.2017.09.028.

[48] Z. Yatabe, J. T. Asubar, and T. Hashizume, "Insulated gate and surface passivation structures for GaN-based power transistors," *J. Phys. D. Appl. Phys.*, vol. 49, no. 39, 2016, doi: 10.1088/0022-3727/49/39/393001.

[49] J. Ma, G. Kampitsis, P. Xiang, K. Cheng, and E. Matioli, "Multi-Channel Tri-gate GaN Power Schottky Diodes with Low ON-Resistance," *IEEE Electron Device Lett.*, vol. 40, no. 2, pp. 275–278, 2018, doi: 10.1109/LED.2018.2887199.

[50] L. Nela, H. K. Yildirim, C. Erine, R. Van Erp, P. Xiang, K. Cheng, and E. Matioli, "Conformal Passivation of Multi-Channel GaN Power Transistors for Reduced Current Collapse," *IEEE Electron Device Lett.*, vol. 42, no. 1, pp. 86–89, 2021, doi: 10.1109/LED.2020.3038808.

[51] C. Erine, J. Ma, G. Santoruvo, and E. Matioli, "Multi-Channel AlGaN/GaN In-Plane-Gate Field-Effect Transistors," *IEEE Electron Device Lett.*, vol. 41, no. 3, pp. 321–324, 2020, doi: 10.1109/LED.2020.2967458.

[52] M. Xiao, Y. Ma, K. Cheng, K. Liu, A. Xie, E. Beam, Y. Cao, and Y. Zhang, "3.3 kV Multi-Channel AlGaN/GaN Schottky Barrier Diodes With P-GaN Termination," *IEEE Electron Device Lett.*, vol. 41, no. 8, pp. 1177–1180, 2020, doi: 10.1109/LED.2020.3005934.

[53] C. Erine, L. Nela, A. Miran Zadeh, and E. Matioli, "Analytical model for multi-channel high-electron-mobility III-N heterostructures," under revision in *AIP Advances*.